Spectroscopy and Rare Decays at CDF

Cheng-Ju S. Lin

(Representing the CDF Collaboration)

Fermi National Accelerator Laboratory, P.O. Box 500, MS 318, Batavia, IL 60510, U.S.A.

Abstract. We report recent results on B hadron mass and rare decay measurements using data collected by the CDF detector in Run II.

INTRODUCTION

The CDF Run II detector [1, 2] has been collecting physics quality data since the beginning of 2002. The upgraded detector and trigger/DAQ system signi£cantly enhanced the physics capability of the experiment. Some of the detector upgrades that are important to heavy ¤avor physics include the extended silicon vertex detector (SVXII), a time-of-¤ight (TOF) system for particle identi£cation, and a new layer of silicon detector (L00) mounted directly on the beam pipe ($r \sim 1.5cm$) for precision vertexing near the interaction point. The brand new trigger system is designed to handle higher beam crossing rate and instantaneous luminosity. One of the new additions to the trigger system is the Silicon Vertex Trigger (SVT). The SVT is able to trigger on hadronic B and charm decays by selecting tracks with large impact parameters. The typical impact parameter resolution for an SVT track is about $48\mu m$ (see Figure 1).

With over 200 pb^{-1} of physics data now on tape, CDF is well positioned to make substantial contribution to the heavy ¤avor physics community. In this paper, we will report recent B hadron mass measurements $(B^+, B^0, B_s, \Lambda_b)$ using exclusively reconstructed decay channels. We will also report on the search for ¤avor changing neutral current (FCNC) decays of $D^0 \to \mu^+\mu^-$ and $B_s \to \mu^+\mu^-$.

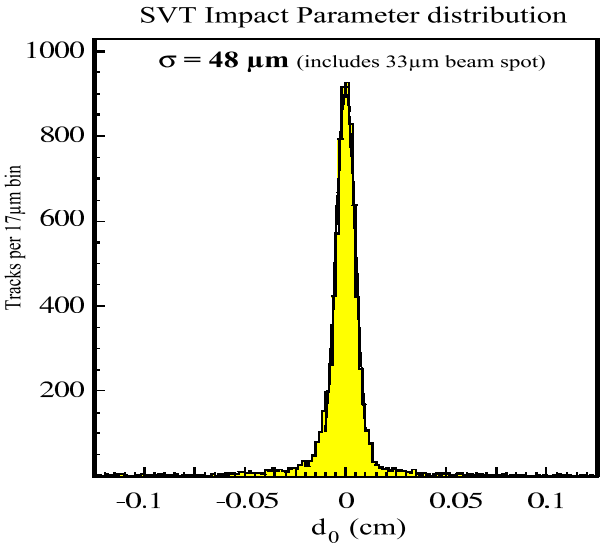

FIGURE 1. Impact parameter distribution of SVT tracks. The £tted impact parameter resolution is $48\mu m$ (includes $33\mu m$ beam spot uncertainty). The typical SVT d_0 cut for displaced track is $\pm 120\mu m$.

SPECTROSCOPY

A good understanding of track parameter corrections due to energy loss is a prerequisite for precision mass measurements. Without proper correction, the measured mass would exhibit a strong p_T dependence. At CDF, a sample of muons from the J/ψ decays are used to calibrate the energy loss correction. Figure 2 shows the J/ψ mass p_T dependence for the various scenarios. The lowest curve shows the p_T dependence without any correction. As expected, the £tted J/ψ mass shows a strong p_T dependence. With the nominal energy loss correction (open triangle), there is still a residual p_T dependence. This residual effect is removed by iteratively tuning the GEANT material description used by the track £tter. Lastly, a global magnetic £eld correction is applied to shift the J/ψ mass to the PDG value (shown in solid circles). The momentum calibration procedure is cross-checked by measuring the mass of K_s, D, Υ, and Ψ'. The measured masses, after applying all corrections, are consistent with the PDG values.

Using $\sim$80 pb^{-1} of data, we have measured the mass of various B hadrons using fully reconstructed J/ψ decay

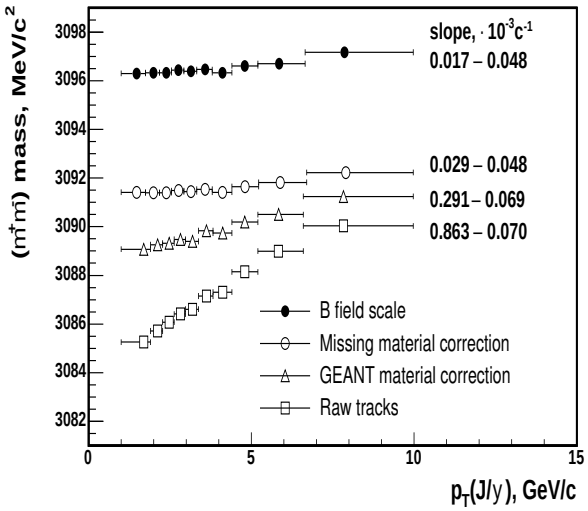

FIGURE 2. The J/psi mass as a function of p_T. The four distributions are: no correction (square box), default energy loss correction (triangle), full energy loss correction (open circle), full energy loss and magnetic £eld corrections (£lled circle).

TABLE 1. Summary of CDF B hadron mass measurements. The £rst quoted error is statistical and the second is systematic.

	Mass (MeV/c^2)	**Data** (pb^-1)
$B^+ \to J/\psi K^+$	$5279.32 \pm 0.68 \pm 0.94$	80
$B^0 \to J/\psi K^{*0}$	$5280.30 \pm 0.92 \pm 0.96$	80
$B_s \to J/\psi\phi$	$5365.50 \pm 1.29 \pm 0.94$	80
$\Lambda_b \to J/\psi\Lambda$	$5280.30 \pm 0.20 \pm 0.96$	70

channels. The reconstructed channels are: $B^+ \to J/\psi K^+$, $B^0 \to J/\psi K^{*0}$, $B_s \to J/\psi\phi$, and $\Lambda_b \to J/\psi\Lambda$. The measured values are shown in Table 1. The invariant mass distributions for B_s and Λ_b candidates are shown in Figure 3 and Figure 4, respectively. The new B_s and Λ_b mass measurements from CDF are the world's best.

At CDF, we have also reconstructed a sample of charged hyperons, Ξ and Ω. The long lived charged hyperons, which have proper lifetimes ($c\tau$) on the order of centimeters, could leave tracks in the inner layers of the CDF silicon vertex detector before decaying. By requiring the pseudo hyperon tracks reconstructed from the decay products to be matched to the silicon track from the parent hyperon, the combinatorial background can be signi£cantly reduced. Figure 5 and 6 show the invariant mass distribution of $\Xi^- \to \Lambda\pi^-$ and $\Omega \to \Lambda K^-$ candidates with the silicon track requirement, respectively. The sample of clean hyperons will be used to reconstruct the bottom-strange baryons: Ξ_b^0, Ξ_b^-, and Ω_b^- to study their production properties.

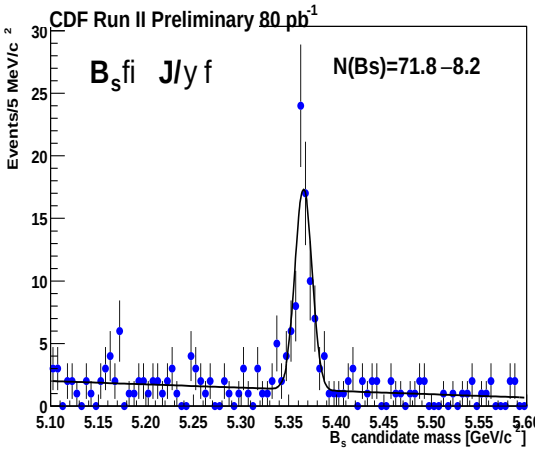

FIGURE 3. The invariant mass distribution for $B_s \to J/\psi\phi$ candidates. The B_s candidate is reconstructed with J/ψ decaying to $\mu^+\mu^-$ and ϕ to K^+K^-.

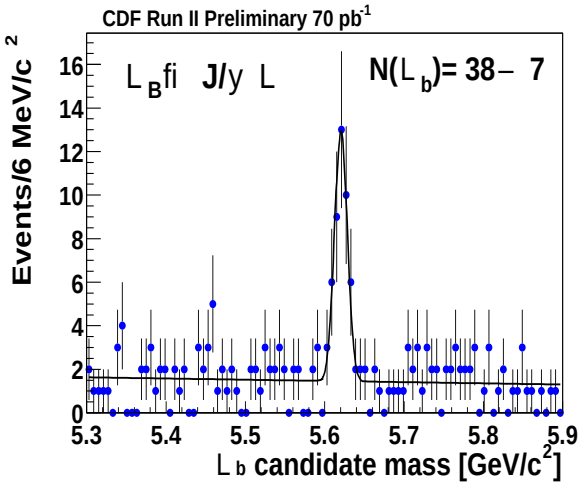

FIGURE 4. The invariant mass distribution for Λ_b candidates. The Λ_b candidate is reconstructed with J/ψ decaying to $\mu^+\mu^-$ and Λ to $p^+\pi^-$.

RARE DECAY ($D^0 \to \mu^+\mu^-$) SEARCH

In the Standard Model, the FCNC decay $D^0 \to \mu\mu$ is heavily suppressed, with an expected branching ratio on the order of 10^{-13}. However, in some R-parity violating SUSY models, the branching ratio could be as large as 10^{-6} [3]. Thus, this decay channel provides a window of opportunity to search for new physics beyond the Standard Model.

The $D^0 \to \mu^+\mu^-$ decays are searched for in the hadronic data sample triggered by the SVT. The measurement is normalized to the decay of $D^0 \to \pi^+\pi^-$, which has similar kinematics as the signal mode and a

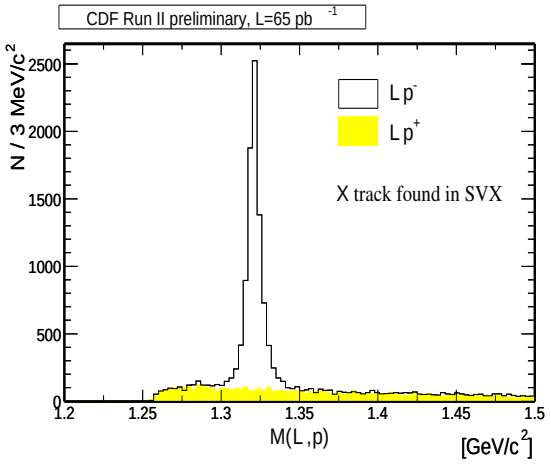

FIGURE 5. The invariant mass distribution for $\Xi \to \Lambda\pi^-$ candidates ($\Lambda \to p^+\pi^-$) with Ξ tracked in the silicon vertex detector. The distribution for the wrong sign candidates is shown in yellow.

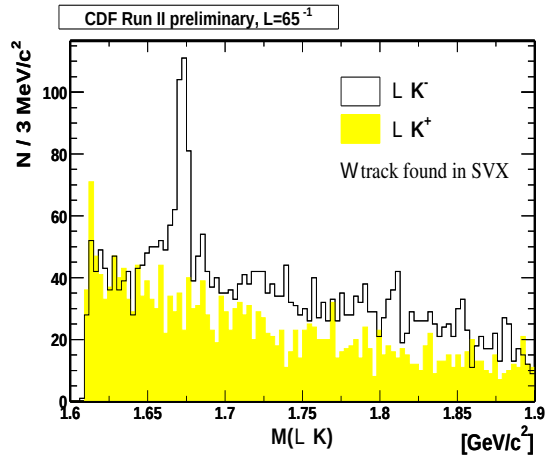

FIGURE 6. The invariant mass distribution for $\Omega \to \Lambda K^-$ candidates ($\Lambda \to p^+\pi^-$) with Ω tracked in the silicon vertex detector. The distribution for the wrong sign candidates is shown in yellow.

well measured branching ratio. To reduce combinatoric backgrounds, the D^0 for both $\mu\mu$ and $\pi\pi$ channels are required to come from $D^{*\pm}$ decay. By using the same track-based trigger for both signal and normalization modes, various ef£ciencies cancel in the relative branching ratio measurement. The remaining main ingredients needed for the measurement are: (1) the number of reconstructed $D^0 \to \pi^+\pi^-$ in the £ducial muon region, (2) the number of signal events (or an upper limit), (3) relative acceptance and reconstruction ef£ciency of $D^0 \to \mu^+\mu^-$ to $D^0 \to \pi^+\pi^-$,and (4) the expected background.

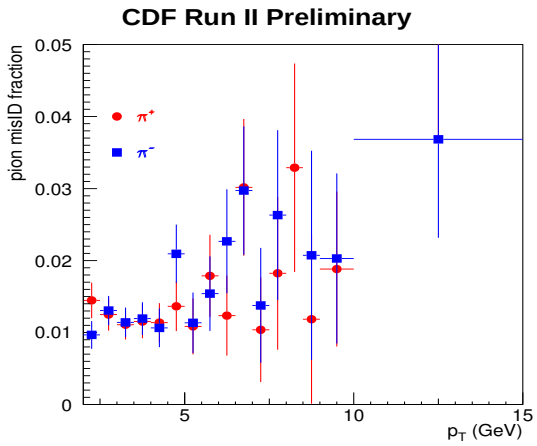

FIGURE 7. The fraction of $\pi^{\pm}$ misidenti£ed as muons vs p_T.

The overall reconstruction ef£ciency ratio, $\varepsilon(\pi\pi)/\varepsilon(\mu\mu)$, is estimated from a combination of measurements and Monte Carlo simulation, as follows. First, $\varepsilon(\mu\mu)$ is obtained by convoluting the p_T spectrum of pions from $D^0 \to \pi^+\pi^-$ with the measured muon reconstruction ef£ciency. To properly account for the effect of hadronic interactions with detector material, $\varepsilon(\pi\pi)$ was estimated from a detailed GEANT detector simulation [4]. Combining the two values, the ef£ciency ratio is found to be 1.13 ± 0.04. The same Monte Carlo simulation used in deriving the reconstruction ef£ciency ratio is also used to determine the geometric acceptance ratio. The geometric acceptance ratio, $\alpha(\pi\pi)/\alpha(\mu\mu)$, is found to be 0.96 ± 0.02. The expected background in the signal mass window has two contributions. The £rst contribution is combinatoric, which can be estimated from the high-mass side-band region. The expected background from this source is 1.6 ± 0.7 events. The second contribution comes from $D^0 \to \pi^+\pi^-$ with both tracks misidenti£ed as muons. The latter contribution can be estimated as the number of $D^0 \to \pi^+\pi^-$ events in the signal mass region (using μ mass hypothesis) times the square of the misidenti£cation probability. The misidenti£cation probability is measured from a sample of $D^0 \to K\pi$ events from tagged $D^{*\pm}$. The $\pi \to \mu$ misidenti£cation probability as a function of p_T is shown in Figure 7. The average $\pi \to \mu$ probability (convoluted with the track p_T spectrum) is about 1.3%. This translates to 0.22 ± 0.02 expected misidenti£cation events. The combined background from the two sources is 1.8 ± 0.7 events.

Based on $69pb^{-1}$ of data, we found no events remaining in the signal region (Figure 8). Using the prescription of Cousins and Highland [5], the limit on the branching

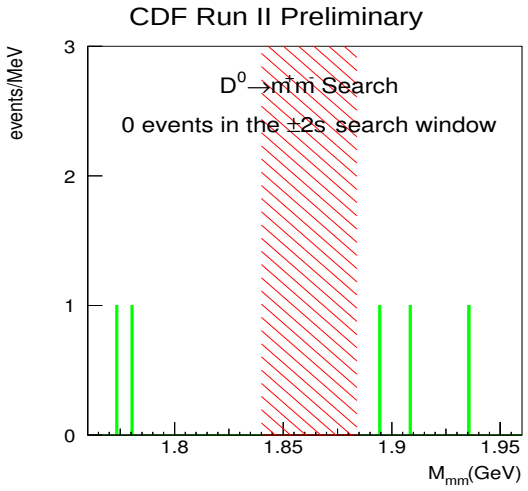

FIGURE 8. The di-muon mass spectrum with $D^{*\pm}$ tag.

ratio is:

- BR($D^0 \to \mu^+\mu^-$)$< 2.4 \times 10^{-6}$ at 90% C.L.
- BR($D^0 \to \mu^+\mu^-$)$< 3.1 \times 10^{-6}$ at 95% C.L.

This result improves the previous published limits from BEATRICE and E771 [6, 7] by about a factor of 2.

RARE DECAY ($B_S \to \mu^+\mu^-$) SEARCH

Similar to $D^0 \to \mu^+\mu^-$, the FCNC decay of $B_s \to \mu^+\mu^-$ is suppressed at the tree level in the Standard Model. The expected branching ratio is $BR(B_s \to \mu^+\mu^-) = 3.8 \times 10^{-9}$. In many SUSY models, this branching ratio can be enhanced to as large as $\sim 10^{-6}$ [8, 9, 10], which would make the decay observable in Run II.

The $B_s \to \mu^+\mu^-$ decays are searched for in the dataset collected by the di-muon trigger. The B_s candidates are require to be in the kinematic £ducial box of $p_T > 6$GeV and rapidity $|y_{B_s}| < 1$. This kinematic box is chosen so that we can readily normalize the result to the measured B production cross-section at the Tevatron. The branching ratio is obtained from the expression:

$$Br(B_s \to \mu^+\mu^-) = \frac{N(B_s \to \mu^+\mu^-)}{2 \cdot \sigma_{B_s} \cdot \mathscr{L}_{total} \cdot \alpha \cdot \varepsilon_{total}}, \quad (1)$$

where N($B_s \to \mu^+\mu^-$) is the number of observed signal events (or upper limit if no signal is observed), σ_{B_s} is the B_s production cross section. The B_s production cross section is obtained by multiplying the measured B_d production cross section [11] by the world average value of f_s/f_d [12]. The uncertainty on σ_{B_s} is the dominant source of systematic uncertainty in this analysis. $\mathscr{L}_{total}$ is the total integrated luminosity. The geometric and trigger acceptance, α, is estimated from the Monte Carlo. The total ef£ciency, ε_{total}, includes tracking, trigger, reconstruction, and analysis cut ef£ciencies. The £rst three ef£ciencies (tracking, trigger and reconstruction) are measured directly from the data. The analysis cut ef£ciency accounts for the ef£ciency of the of¤ine analysis cuts used in the optimization. The four primary discriminating variables that we use to optimize the analysis are: the invariant of the muon pair ($M_{\mu\mu}$), the proper lifetime of the B_s candidate ($c\tau$), the 2-D (transverse plane) opening angle between the B_s momentum vector and the decay vertex axis ($\Delta\phi$), and the isolation cut (Iso). The isolation variable is de£ned as $Iso = p_T(B_s)/(p_T(B_s) + \Sigma p_T(trk_i))$, where the summation is over all tracks within a cone of $\sqrt{\Delta\eta^2 + \Delta\phi^2} < 1$ about the B_s momentum direction. The analysis cut ef£ciency is estimated from the Monte Carlo and cross-checked using a sample of $B^+ \to J/\psi K^+$ events from the data.

The number of background events remain in the signal region is estimated from Monte Carlo and data. From the Monte Carlo study, we concluded that contamination from resonant decays (eg. $B \to h^+h^-$) are negligible at the current level of sensitivity. The dominant source of background comes from combinatorics. We have estimated the combinatorial background from mass side-bands. To improve the estimate, we factorize the expected rejection for each (non-correlated) group of cuts separately. The total background is obtained from the expression: $N_{bkg} = N_{SB}(c\tau, \Delta\phi) \cdot R_{Iso} \cdot R_{mass}$, where $N_{SB}(c\tau, \Delta\phi)$is the number of sideband events passing a given set of $c\tau$ and $\Delta\phi$ cuts, R_{Iso} is the expected rejection for a given Iso cut, and R_{mass} is the expected rejection for a given mass window cut. The variables $c\tau$ and $\Delta\phi$ are correlated and therefore cannot be treated separately. The resulting total background is estimated to be 0.54 ± 0.2 events.

The di-muon invariant mass spectrum (using $113 pb^{-1}$ of data) with the £nal selection cuts are shown in Figure 9. There is one event within the B_s search window. Given the observation is consistent with background expectation, we calculate the upper limit on the branching ratio using the method of reference [13]. The resulting limits are:

- BR($B_s \to \mu^+\mu^-$)$< 9.5 \times 10^{-7}$ at 90% C.L.
- BR($B_s \to \mu^+\mu^-$)$< 1.2 \times 10^{-6}$ at 95% C.L.

This result is a factor of 2 better than the published limit [14].

We have extended the analysis to search for $B_d \to \mu^+\mu^-$ decays. The analysis procedure is identical to the B_s search. The event in the B_s mass window also falls in the B_d search window. Given the observation

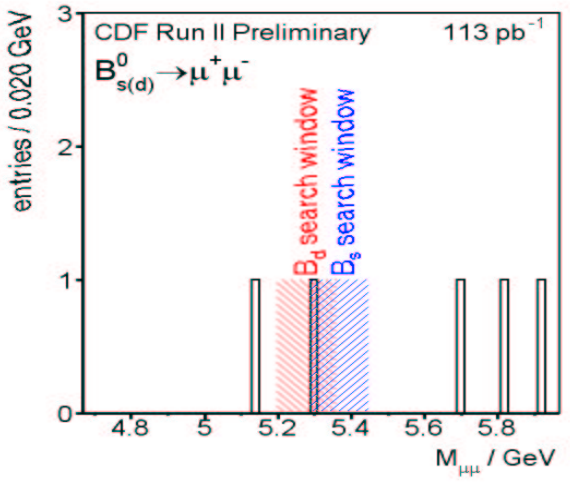

FIGURE 9. The di-muon mass spectrum. The 3σ mass search window for B_s is shown in the blue hatched region. The 3σ mass search window for B_d is shown in the red hatched region. There is one event overlapping both search windows.

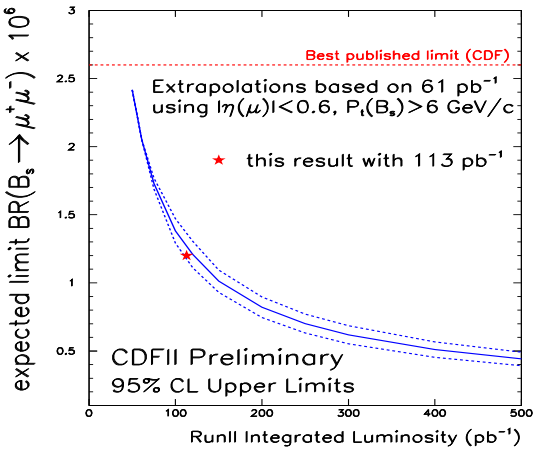

FIGURE 10. The expected 95% C.L. upper limit on BR($B_s \to \mu^+\mu^-$) as a function of integrated luminosity.

is also consistent with background expectation ($N^{Bd}_{bkg} = 0.59 \pm 0.22$), we set an upper limit on the branching ratio:

- BR($B_d \to \mu^+\mu^-$)$< 2.5 \times 10^{-7}$ at 90% C.L.
- BR($B_d \to \mu^+\mu^-$)$< 3.1 \times 10^{-7}$ at 95% C.L.

Figure 10 shows the expected sensitivity of $B_s \to \mu^+\mu^-$ search as a function of integrated luminosity. In the absence of a signal, with twice the data and no improvement in the analysis technique, the limit is expected to improve by another factor of two.

SUMMARY

The Run II physics program is now well underway. Using only a fraction of the available data, CDF has already made world class measurements in the area of heavy ¤avor physics. In this paper, we presented some preliminary measurements on B hadron masses and rare decay searches. Some of which are already the best in the world. With more data on the way, the prospect of performing precision spectroscopy on the broad spectrum of hadrons produced (including B_c, charm-strange and bottom-strange baryons, etc...) at the Tevatron is very promising. CDF will also remain competitive in the area of rare decay measurements.

REFERENCES

1. Abe, F., et al., *Nucl. Instr. Meth.*, **A271**, 387–403 (1988).
2. CDF II Collaboration, *FERMILAB-PUB-96-390-E* (1996).
3. Burdman, G., Golowich, E., Hewett, J., and Pakvasa, S., *Phys. Rev.*, **D66**, 014009 (2002).
4. Brun, R., Hagelberg, R., Hansroul, M., and Lassalle, J. C., *CERN-DD-78-2-REV and CERN-DD-78-2* (1978).
5. Cousins, R. D., and Highland, V. L., *Nucl. Instrum. Meth.*, **A320**, 331–335 (1992).
6. Adamovich, M., et al., *Phys. Lett.*, **B408**, 469–475 (1997).
7. Alexopoulos, T., et al., *Phys. Rev. Lett.*, **77**, 2380–2383 (1996).
8. Dedes, A., Dreiner, H. K., Nierste, U., and Richardson, P. (2002).
9. Baer, H., et al., *JHEP*, **07**, 050 (2002).
10. Arnowitt, R., Dutta, B., Kamon, T., and Tanaka, M., *Phys. Lett.*, **B538**, 121–129 (2002).
11. Acosta, D., et al., *Phys. Rev.*, **D65**, 052005 (2002).
12. Preliminary estimate from PDG Heavy Flavor Average Group, *http://www.slac.stanford.edu/xorg/hfag/osc/PDG_2003/index.html* (2003).
13. Feldman, G. J., and Cousins, R. D., *Phys. Rev.*, **D57**, 3873–3889 (1998).
14. Abe, F., et al., *Phys. Rev.*, **D57**, 3811–3816 (1998).